NeuroToxicology 40 (2014) 65–74

Contents lists available at ScienceDirect

NeuroToxicology

Nicotinamide adenine dinucleotide prevents neuroaxonal degeneration induced by manganese in cochlear organotypic cultures

Lu Wang [a,b], Dalian Ding [b,d], Richard Salvi [b], Jerome A. Roth [c,*]

[a] Department of Otolaryngology, Head and Neck Surgery, The Third Xiangya Hospital, Central South University, Changsha, Hunan 410013, China
[b] Center for Hearing and Deafness, University at Buffalo, Buffalo, NY 14214, United States
[c] Department of Pharmacology and Toxicology, University at Buffalo, Buffalo, NY 14214, United States
[d] Department of Otolaryngology, Head and Neck Surgery, Xiangya Hospital, Central South University, Changsha, Hunan 410008, China

ARTICLE INFO

Article history:
Received 9 September 2013
Accepted 25 November 2013
Available online 3 December 2013

Keywords:
Manganese
Ototoxicity
NAD
Spiral ganglion neurons
Hair cells
Apoptosis

ABSTRACT

Manganese (Mn) is an essential trace mineral for normal growth and development. Persistent exposures to high atmospheric levels of Mn have deleterious effects on CNS and peripheral nerves including those associated with the auditory system. Nicotinamide adenine dinucleotide (NAD) is a coenzyme which functions in the electron transfer system within the mitochondria. One of the most notable protective functions of NAD is to delay axonal degenerations caused by various neurodegenerative injuries. We hypothesized that NAD might also protect auditory nerve fibers (ANF) and SGN from Mn injury. To test this hypothesis, cochlear organotypic cultures were treated with different doses of Mn (0.5–3.0 mM) alone or combined with 20 mM NAD. Results demonstrate that the percentage of hair cells, ANF and SGN decreased with increasing Mn concentration. The addition of 20 mM NAD did not significantly reduce hair cells loss in the presence of Mn, whereas the density of ANF and SGN increased significantly in the presence of NAD. NAD suppressed Mn-induced TUNEL staining and caspase activation suggesting it prevents apoptotic cell death. These results suggest that excess Mn has ototoxic and neurotoxic effects on the auditory system and that NAD may prevent Mn-induced axonal degeneration and avoid or delay hearing loss caused by excess Mn exposure.

1. Introduction

Manganese (Mn) is an essential trace metal required for normal growth and development and cellular homeostasis. Mn serves as a discrete cofactor for many enzymes including glutamine synthetase, superoxide dismutase, and pyruvate carboxylase (Rivera-Mancia et al., 2011). However, excessive exposure to Mn is linked with a severe and debilitating disorder known as manganism (Olanow et al., 1996; Pal et al., 1999). Manganism usually results from extended occupational exposure to Mn (e.g., Mn miners, welders, and individuals living near ferroalloy plants and battery factories) and decreased Mn excretion in diseased liver (Bouchard et al., 2007; Bowler et al., 2007; Lucchini et al., 2000, 2007). Symptoms of manganism are characterized by extrapyramidal disturbances similar to those seen in Parkinson's disease (Dobson et al., 2004); however, manganism deviates from Parkinsonism in its early clinical stages including differences in behavioral and cognitive function, symmetrical effects, milder tremors at rest, little or no response to L-DOPA, and prominent histological damage to the globus pallidus rather than substantia nigra pars compacta (Calne et al., 1994; Olanow, 2004; Pal et al., 1999). Recent studies have further suggested that Mn may have deleterious effects on hearing. Studies in our laboratory using cochlear organotypic cultures isolated from rats showed that Mn produced significant damage to peripheral auditory nerve fibers, the sensory hair cells (more toxic to inner hair cells than outer hair cells), and SGN (Ding et al., 2011). Sensory hair cells were slightly more resistant to Mn toxicity than the auditory nerve fibers.

Management of Mn-induced ototoxicity has yet to be established; however by understanding the mechanisms of damage may facilitate the development of new therapeutic strategies. It is generally accepted that Mn promotes cell death via degeneration of mitochondria leading to apoptosis. Mitochondrial dysfunction is brought about by excess accumulation of Ca^{2+} produced by Mn inhibition of sodium-dependent and sodium-independent Ca^{2+} exporters within the mitochondria (Gavin et al., 1992, 1999; Gunter et al., 2006). This subsequently results in uncoupling of the respiratory chain and activation of the permeability transition pore (PTP) allowing diffusion of low-molecular weight solutes into the mitochondria resulting in its swelling and the subsequent loss of cytochrome c. Ultimately, this leads to the generation of reactive oxygen species (ROS) which subsequently activates many of the

* Corresponding author at: Department of Pharmacology and Toxicology, University at Buffalo, 11 Cary Hall, Buffalo, NY 14214, United States.
Tel.: +1 716 829 3236; fax: +1 716 829 2801.
E-mail address: jaroth@buffalo.edu (J.A. Roth).

0161-813X/$ – see front matter © 2013 Elsevier Inc. All rights reserved.
http://dx.doi.org/10.1016/j.neuro.2013.11.007

classical signaling pathways associated with programmed cell death including increased TUNEL staining, internucleosomal DNA cleavage, activation of the JNK and p38 pathways (stress activated protein kinase) and activation of caspase-3 (Chun et al., 2001; Desole et al., 1996, 1997; Hirata et al., 1998; Latchoumycandane et al., 2005; Roth et al., 2000; Schrantz et al., 1999). In addition, Mn also interferes with oxidative phosphorylation by inhibiting both mitochondrial F1-ATPase (Gavin et al., 1992, 1999) and complex I (Galvani et al., 1995) leading to the depletion of ATP (Chen and Liao, 2002; Roth et al., 2000). Consistent with the fact that Mn-induced cell death involves oxidative stress is the observation that treatment with antioxidants can prevent Mn toxicity (Migheli et al., 1999).

Oxidized and reduced forms of NAD serve as coenzyme in all living cells and can be synthesized in the human body from tryptophan and aspartic acid or supplemented in vivo via intake of niacin, which is commonly used as a dietary supplement and is easily accessible to the general public (Belenky et al., 2007). Besides involvement in redox reactions within the mitochondria, NAD is also utilized in metabolic events including ADP-ribosylation, poly (ADP-ribose) polymerization, cADP-ribose synthesis, and sirtuins, a group of enzymes that function primarily in reversing acetyl modifications of lysine on histones and other proteins (Sauve, 2008). Several studies have found that NAD can delay axonal degenerations caused by various diseases, including traumatic brain injury, ischemia damage, autoimmune encephalomyelitis, p53-induced neuron apoptosis, and radiation-induced immunosuppression (Belenky et al., 2007; Sauve, 2008). Although Mn has been found to damage the neurons and sensory cells in the inner ear, no studies have been conducted to explore the possibility that NAD may protect against Mn ototoxicity. Since NAD can attenuate mitochondrial oxidative damage in rat brain, we hypothesized that it would prevent ototoxicity induced by excessive exposure to Mn. Thus, using the Mn ototoxicity model of rat cochlear organotypic cultures as reported in our previous study (Ding et al., 2011), we explored the in vitro protective effects of NAD on sensory hair cells (HC), auditory nerve fibers (ANF), and SGN.

2. Materials and methods

2.1. Animal subjects

Postnatal day 3 SASCO Sprague-Dawley rats purchased from Charles River Laboratories were used for this study. The experiments were carried out according to the National Institutes of Health Guidelines for the Care and Use of Laboratory Animals and approved by the University at Buffalo Animal Care and Use Committee.

2.2. Cochlear organotypic cultures, $MnCl_2$ and NAD

Rat cochlear organotypic cultures were prepared as described previously (Ding et al., 2002; McFadden et al., 2003). The cochleae were carefully dissected out and the whole basilar membrane containing the organ of Corti, auditory nerve fibers and SGN were transferred onto rat tail collagen gel in the culture dish (Type 1 collagen, 3.76 mg/ml in 0.02 N acetic acid, 10× basal medium Eagle, 2% sodium carbonate, 9:1:1 ration). Serum-free culture medium (1.3 ml, 0.01 g/ml bovine serum albumin [Sigma A-4919], 1% Serum-Free Supplement [Sigma I-1884], 2.4% of 20% glucose, 0.2% Penicillin G, 1% 200 mM glutamine, 95.4% 1× basal medium Eagle [Sigma B-1522]) was added to each culture dish. The whole basilar membrane prepared as a flattened preparation was placed on the surface of the collagen gel and then maintained in an incubator (37 °C, 5% CO_2) overnight. On the second day, the culture medium was removed and exchanged with fresh medium plus the desired compounds specific for each experimental protocol. The cultures were exposed to various concentrations of $MnCl_2$ in the presence or absence of 20 mM NAD and incubated for various times at 37 °C in 5% CO_2. The concentrations of Mn used in these experiments were selected to be comparable to that employed in our laboratory (Ding et al., 2011; Lin et al., 1993) and others (Giordano et al., 2009; Hernandez et al., 2011; Rovetta et al., 2007) using a variety of cell cultures systems. The concentration of NAD employed in this paper are similar to that used previously to examine protection against neuronal degeneration (Wang et al., 2005) and cell death (Alano et al., 2004; Ding et al., 2012; Ying et al., 2003).

2.3. Staining: auditory nerve and cochlear hair cells

Cells were removed from the culture dishes at the end of each treatment, fixed for 2 h in 10% formalin at room temperature, and rinsed three times in 0.1 M phosphate buffered saline (PBS). As described in our previous publications (Ding et al., 2002; McFadden et al., 2003, #3192), specimens were immersed in a monoclonal primary antibody against neuronal class III β-tubulin (Covance, MMS-435P) and diluted in 1% Triton X-100 and 5% goat serum in 0.1 M PBS for 48 h at 4 °C. Afterward, specimens were rinsed three times with 0.1 M PBS and incubated for 2 h at room temperature in a second antibody conjugated with Cy3 (goat anti-mouse IgG, Jackson ImmunoResearch). Specimens were subsequently rinsed three times with 0.1 M PBS and labeled with phalloidin conjugated with Alexa Fluor488 (Invitrogen A12379, diluted in 1% Triton X-100, 5% goat serum in 0.1 M PBS, 1 h at room temperature). After rinsing three times with 0.1 M PBS, specimens were mounted on glass slides in glycerin and coverslipped. To quantify the neurotoxic effect of Mn on SGN and the protection by NAD, the number of β-tubulin labeled SGN were counted in a 141.4 μm × 141.4 μm × 5 μm volume from 8 cochlear cultures (3 locations in each cochlear culture).

2.4. Cochleograms

Cochleograms were prepared from cochlea cultures as described previously (Wei et al., 2010). Cochlear hair cells (HC) stained with Alexa Fluor488 phalloidin were examined under a fluorescent microscope (Zeiss Axioskop, 400×) with the appropriate filter. Using previously established methods, the numbers of missing hair cells were counted over 0.24 mm intervals along the entire length of the organ of Corti from apex to base (Deng et al., 2013; Wei et al., 2010). Using laboratory norms from control animals (Ding et al., 2007) and custom software, cochleograms were used to show the percent viable of inner hair cells (IHC) and outer hair cells (OHC) as a function of the distance from the apex of the cochlea for each treatment condition as described above (Ding et al., 2007). Results from eight samples were averaged to obtain the mean cochleogram from each experimental group.

2.5. TUNEL staining

To evaluate DNA strand breaks for cells undergoing apoptosis, specimens were labeled for TUNEL (terminal deoxynucleotidyl transferase biotin-dUPT nick end labeling) using the APO-BrdU TUNEL Assay Kit (Invitrogen A23210) following the manufacturer's protocol. Nine hours following treatment with 1.0 mM Mn in the presence or absence of 20 mM NAD, the specimens were fixed with formalin as described above. Specimens were transferred to ice-cold 70% ethanol overnight in a −20 °C freezer and subsequently rinsed twice in washing buffer. Afterwards, specimens were immerged in 100 μl DNA-labeling solution (20 μl reaction buffer,

1.5 μl TdT enzyme, 16 μl BrdUTP, 62.5 μl dH_2O) for 8 h at 37 °C and washed twice in rinse buffer. Specimens were subsequently incubated in 100 μl antibody staining solution (5.0 μl, Alexa 488 labeled anti-BrdU antibody, 95 μl rinse buffer) for 1 h at room temperature and rinsed once with 0.1 M PBS. Afterwards, specimens were mounted on glass slides in glycerin and coverslipped.

2.6. Caspase staining

To detect activated caspases in SGN undergoing apoptosis, specimens were labeled with CaspGLOW Red Active caspase-3, caspase-8 and caspase-9 Staining Kits (BioVision) as described previously (Deng et al., 2013). Six hours following treatment with 1.0 mM Mn in the presence or absence of 20 mM NAD, the unfixed specimens were labeled for the active forms of caspase-3, caspase-8 and caspase-9 following the manufacturer's instructions. Specimens were subsequently rinsed twice with wash buffer and fixed for 2 h in 10% formalin at room temperature and then rinsed three times in 0.1 M PBS. As described above, specimens were stained with class III β-tubulin and incubated in a secondary antibody conjugated with Alexa Fluor 488. After rinsing three times with 0.1 M PBS, specimens were mounted on glass slides in glycerin and coverslipped.

2.7. Confocal microscopy

Cochlea specimens were examined under a confocal microscope (Zeiss LSM-510 meta, step size 0.5 μm per slice) using filters appropriate to detect the red fluorescence of Cy3 (excitation 550 nm, emission 570 nm), green fluorescence of Alexa Fluor 488 (excitation 488 nm, emission 520 nm), and red fluorescence for caspase-3, caspase-8 or caspase-9 (excitation 540 nm, emission 570 nm). Images from multiple layers were typically merged into a single plane using Advanced Imaging Microscopy (version 4.0, Carl Zeiss) and photomicrographs were edited with Adobe Photoshop (version CS5.0) as described previously (Ding et al., 2002).

3. Results

3.1. Mn damages cochlear organotypic cultures

Initial studies were performed to characterize the damage in HC, ANF and SGN from the upper middle turn of the cochlea in specimens cultured for 48 h with and without $MnCl_2$. Results from control cultures are illustrated in Fig. 1A. Strong Alexa Fluor 488 phalloidin staining of actin was present in both the cuticular plate and stereocilia of HC. The three rows of OHC and single row of IHC were arranged in orderly rows and there was no hair cell loss or damage. The peripheral ANF and SGN were labeled with β-tubulin and Cy3 conjugated secondary antibody. The ANF of the SGN radiating outward toward the IHC and OHC were organized into smooth, thick fascicles. Normal SGN have large and oval-shaped soma. Fig. 1B illustrates the degenerative changes after 48 h treatment with 3.0 mM Mn. Most OHC, IHC, ANF and SGN were missing. The remaining ANFs were fragmented and thin. The soma of the remaining SGN were shrunken and condensed, features characteristic of cells undergoing apoptosis.

3.2. Effect of Mn concentration and protection by NAD

Fig. 2A–C shows the effect of various Mn concentrations ranging from 0.5 mM to 3.0 mM on cochlear organotypic cultures after 48 h exposure. At the lowest concentration of Mn (0.5 mM), the OHC appeared normal but the IHC and ANF started to decline when compared to the data shown in Fig. 1A for non-treated cultures. At the higher concentrations of Mn, the density of HC, ANF and SGN were further decreased. The actin in the cuticular plate and the stereocilia of the single row of IHC and three rows of OHC were also reduced and the ANF started to appear thin and fragment. SGN soma were shrunken and fragmented. Take together these confocal photomicrographs clearly illustrate a dose-dependent deleterious effect of Mn on cochlear HC, SGN and ANF. In comparison, Fig. 2D–F shows cochlear cultures treated with various concentrations of Mn combined with 20 mM NAD. At the two lowest concentrations of Mn employed, NAD clearly prevented the toxic actions of Mn. Quantification of the protective effects of NAD are presented by the data which follows.

3.3. Cochleograms

To evaluate the toxic effects of Mn and the protective effect of NAD, cochleograms (n = 8/group) measuring the percentage loss of IHC and OHC as a function of the percent distance from the apex of the cochlea were calculated 48 h after treatments with various concentrations of Mn alone or Mn combined with 20 mM NAD. At the lowest dose of Mn (0.5 mM), there was no observable OHC loss (Fig. 3B) consistent with non-treated controls (Fig. 3A); likewise there was no OHC loss with 0.5 mM Mn plus 20 mM NAD (Fig. 3E).

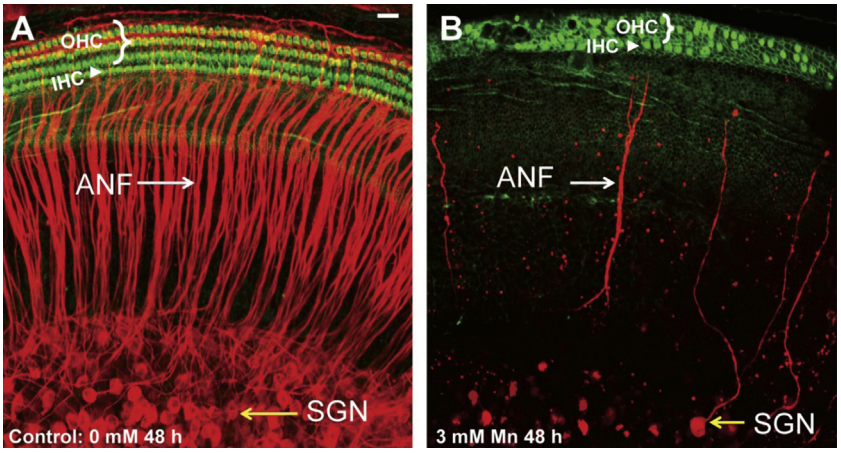

Fig. 1. Representative confocal photomicrographs show cochlear organotypic cultures from upper middle of the cochlea after 48 h treatment without Mn (A) and with 3 mM Mn (B). Alexa Fluor488 phalloidin (green fluorescence) labels three rows of outer hair cells (OHC) and one row of inner hair cells (IHC). Antibody against neuronal class III β-tubulin plus Cy3 conjugated secondary antibody (red fluorescence) labels auditory nerve fibers (ANF) and spiral ganglion neurons (SGN). White brackets show three rows of OHC; arrowhead shows single row of IHC. White arrow points to bundles of ANF radiating out from the SGN (yellow arrow) toward the HC. Scale bar in (A): 25 μm. (For interpretation of the references to color in this figure legend, the reader is referred to the web version of the article.)

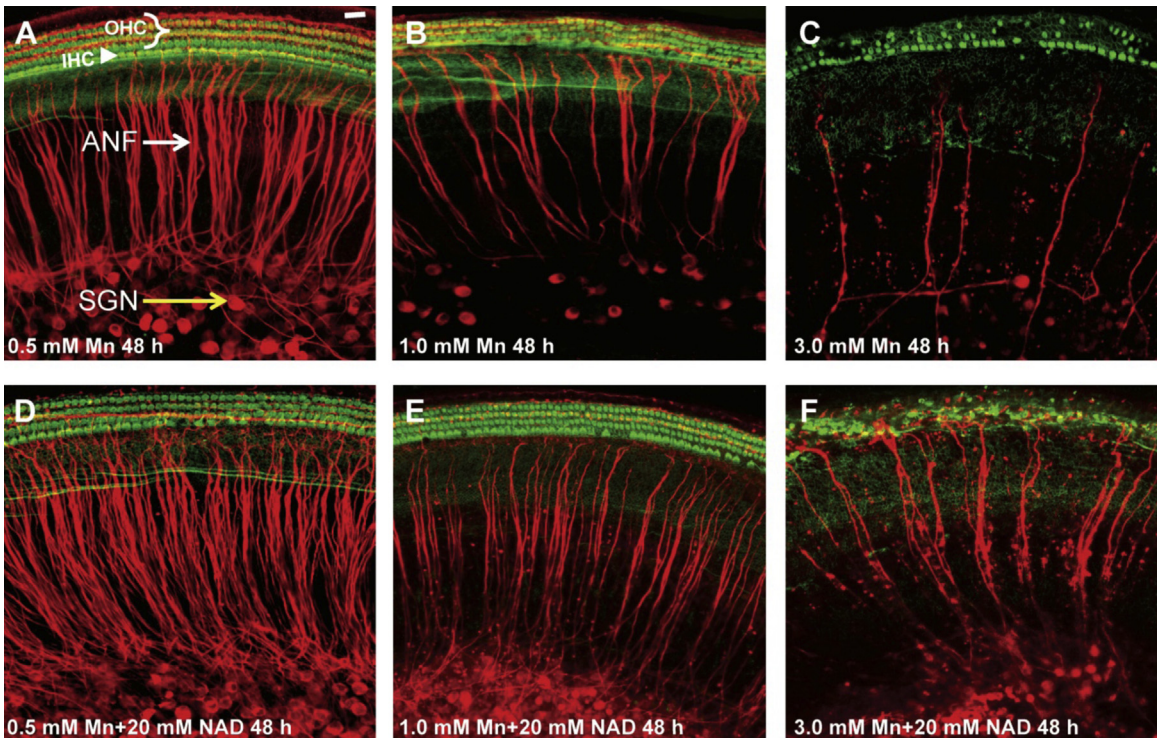

Fig. 2. Representative confocal images show cochlear organotypic cultures from upper middle turn of the cochlea after 48 h treatment with various concentrations of Mn (A)–(C) alone or combined with 20 mM NAD (D)–(F). Alexa Fluor488 phalloidin (green fluorescence) labels hair cells (HC) and antibody against neuronal class III β-tubulin and Cy3 conjugated secondary antibody (red fluorescence) labels auditory nerve fibers (ANF) and spiral ganglion neurons (SGN). White bracket shows three rows of OHC and arrowhead shows the single row of IHC. White arrow points bundles of ANF fascicles radiating out from the SGN toward the IHC and OHC. Yellow arrow points to SGN soma. Scale bar in (A): 25 μm. Note partial loss of ANF and SGN with 1 mM Mn (B); treatment with 3 mM Mn resulted in almost complete loss of ANF plus partial loss of IHC and OHC (C). Treatment with 20 mM NAD protected ANF and IHC and OHC from 1 mM (panel E vs. B) and 3 mM (panel F vs. C) from Mn-induced damage. (For interpretation of the references to color in this figure legend, the reader is referred to the web version of the article.)

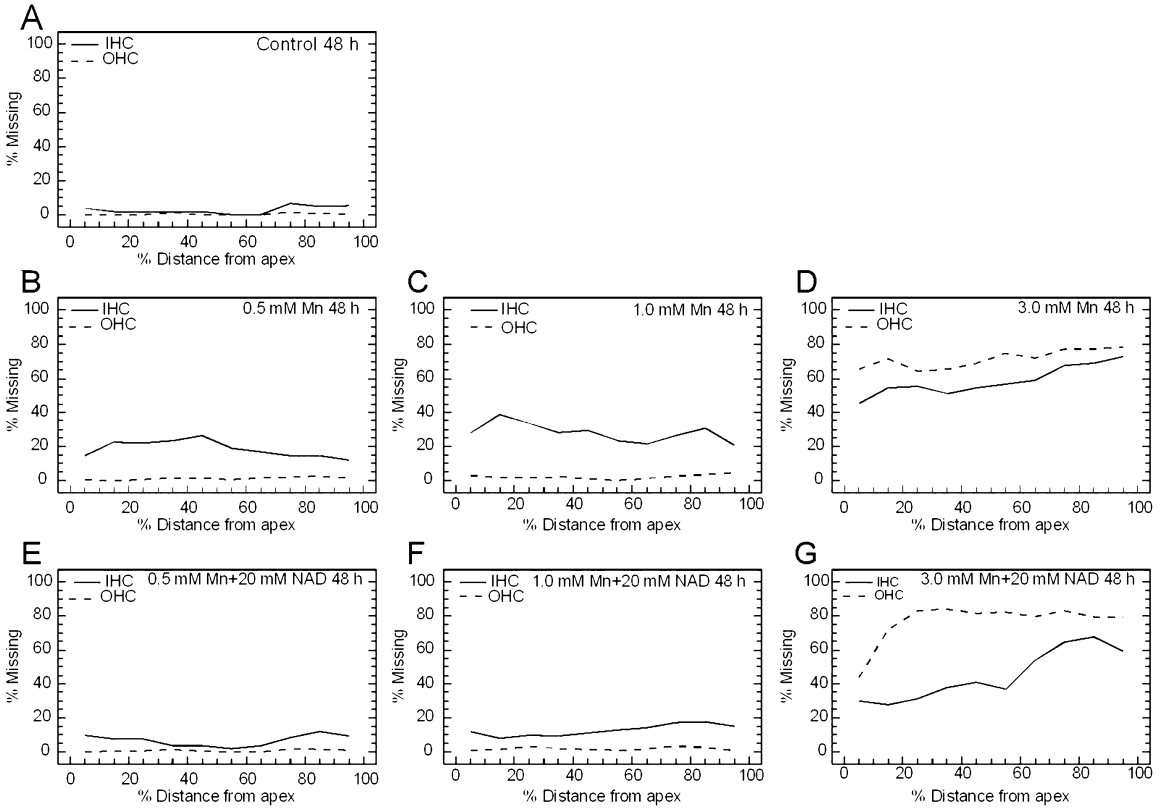

Fig. 3. Mean cochleograms ($n = 8$) showing the percent of missing IHC (solid line) and OHC (dashed line) versus percent distance from the apex of the cochlea. (A) Controls culture for 48 h. Cochleae cultured for 48 h with 0.5, 1.0 or 3.0 mM of Mn alone (B)–(D) or Mn plus 20 mM NAD.

In contrast, there was approximately a 20% loss of IHC with 0.5 mM Mn alone (Fig. 3B), however, the IHC loss decreased to less than 10% with the combination of 0.5 mM Mn plus 20 mM NAD (Fig. 3E). There was also little or no OHC loss with 1.0 mM Mn alone (Fig. 3C) or in combination with NAD (Fig. 3F). However, IHC loss increased to approximately 30% with 1.0 mM Mn alone (Fig. 3C); the IHC loss decreased to 10–20% when 20 mM NAD was combined with the Mn (Fig. 3F). When compared to the lower concentrations of Mn, the highest concentration (3.0 mM) resulted in a greater loss of OHC (~70%) compared to that of the IHC (~55%) over most of the cochlea (Fig. 3D). As to why this change in sensitivity occurred at the highest concentration of Mn is not known but is consistent with the difference in response to 20 mM NAD which failed to reduce OHC loss, but was capable of producing a partially reduction in IHC damage mainly in the apical portion of the cochlea (Fig. 3G).

3.4. Mn damages ANF and protection by NAD

The data presented in Fig. 4 show the condition of ANF in the upper middle turn of the cochlea after 48 h for control cultures (Fig. 4G) and those treated with various concentrations of Mn alone (Fig. 4A–C) or combine with 20 mM NAD (Fig. 4D–E). The normal controls displayed smooth, thick fascicles of ANF which radiate out from the SGN toward the HC (Fig. 4G). With increasing doses of Mn, the number of surviving ANF decreased, the fascicles became thinner and blebbing and fragmentation of ANFs increased (Fig. 4A–C). The addition of 20 mM NAD to the Mn treated cultures resulted in a substantial increase in ANF survival along with reduced blebbing and fragmentation of the fibers (Fig. 4D–F). However, under these conditions, NAD only partially prevented ANF damage since blebbing and fragmentation were still evident at the highest Mn concentration (Fig. 4F).

To quantify the neurotoxic effect of Mn on ANF and the protective effects of NAD, we counted the number of surviving ANF per 0.25 mm longitudinal distance in the upper middle turn of the cochlea. Fig. H shows the mean ($n = 48$/group) numbers of ANF/0.25 mm in control cochleae and cochleae treated for 48 h with various concentration of Mn alone or Mn plus 20 mM NAD. In control cultures, approximately 102 fibers/0.25 mm were present. There was a statistically significant effect of treatment (one-way ANOVA, $p < 0.0001$, $F = 285.6$, 8 df). The mean numbers of ANF in the groups treated with 0.5, 1 and 3 mM Mn alone were significantly (Newman–Keuls, $p < 0.05$, downward blue arrows) less than in the control group. The mean numbers of fibers in the 0.5 mM Mn group was significantly different from the 1 mM group and the 1 mM Mn group was similarly significantly different from the 3 mM group (Newman–Keuls, $p < 0.05$, horizontal blue arrow). Combined treatment with Mn plus 20 mM NAD significantly increased ANF survival compare to groups treated with Mn alone (Newman Keuls, $p < 0.05$, horizontal red bar).

3.5. Mn damages SGN and protection by NAD

Fig. 5 displays a representative confocal image of SGNs from the upper middle turn of the cochlea of control cultures and cultures treated for 48 h with varying concentrations of Mn or Mn plus 20 mM NAD. Normal SGNs have a large round soma and the cytoplasm is heavily immunolabeled with class III β-tubulin with the exception of the nucleolus (Fig. 5G). As the Mn concentrations increase, the SGN soma and nucleolus shrank in size, soma shape became irregular and the number of SGN decreased (Fig. 5A–C). In cultures treated with various concentrations of Mn plus 20 mM NAD, soma and nucleolus shrinkage and SGN losses were less severe than in cultures treated with a similar concentration on Mn alone (Fig. 4D–F vs. A–C). To quantify the neurotoxic effect of Mn

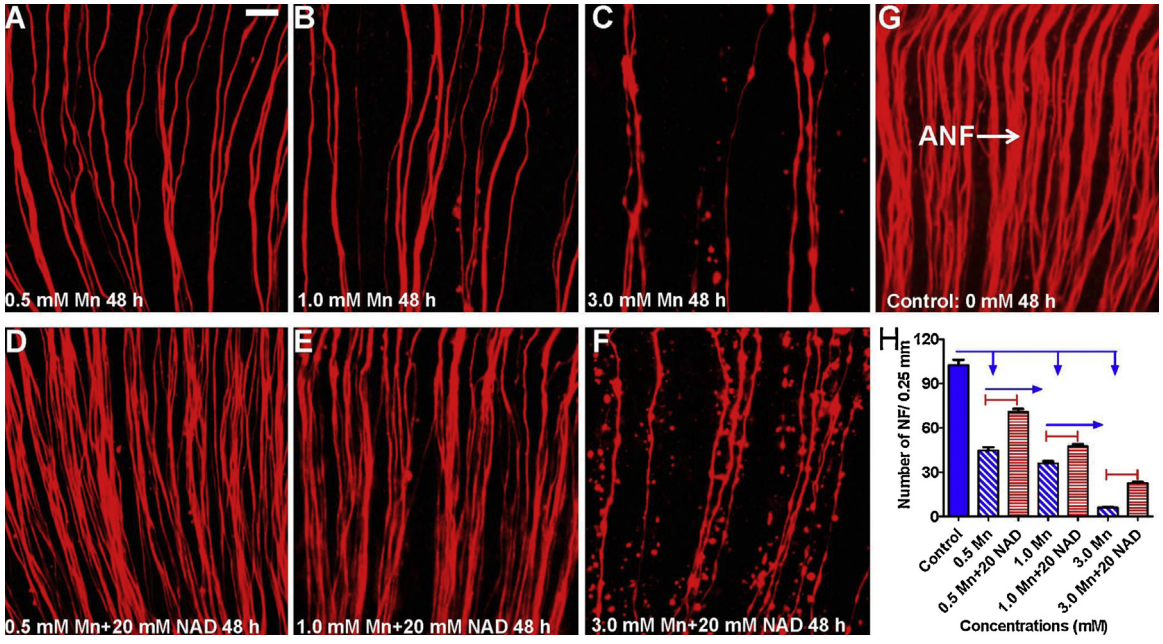

Fig. 4. Representative confocal images showing the condition of the peripheral auditory nerve fibers (ANF) radiating out from the SGN toward the HC. Images from upper middle turn of the cochlea after 48 h in culture with Mn alone ((A)–(C); 0.5 to 3 mM), Mn ((D)–(F); 0.5–3 mM) plus 20 mM NAD or untreated controls (G). ANF labeled with antibody against neuronal class III β-tubulin and Cy3 conjugated secondary antibody. White arrow points bundles of ANF (G). Scale bar in (A): 20 μm. (H) Mean ($n = 48$) numbers of ANF/0.25 mm measured in upper middle turn of the cochlea after 48 h in culture; data shown for controls and those treated with various concentrations of Mn alone or the combination of Mn plus 20 mM NAD. Downward blue arrows show Mn conditions that were significantly different from control ($p < 0.05$). Horizontal blue arrows show Mn conditions that were significantly different from next higher concentration ($p < 0.05$). Horizon red bars show conditions with Mn + NAD that were significantly ($p < 0.05$) different from Mn of the same concentration. (For interpretation of the references to color in this figure legend, the reader is referred to the web version of the article.)

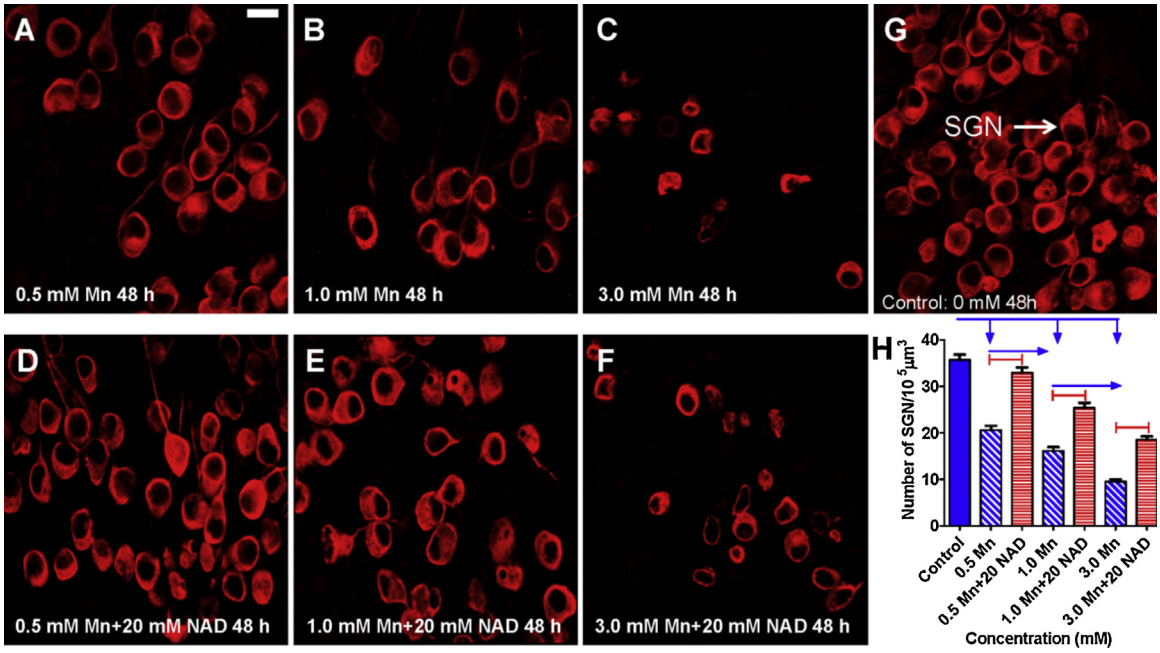

Fig. 5. Representative confocal images showing SGN from upper middle turn of the cochlea after 48 h in culture in the absence of Mn (G) or with treatment with various concentrations of Mn alone (A) and (B) or Mn plus 20 mM NAD (D)–(F). SGN were labeled with antibody against neuronal class III β-tubulin and Cy3 conjugated secondary antibody. White arrow (G) points to soma of SGN. Scale bar in (A): 10 μm. (H) Mean (n = 24) density of SGN/10^5 μm^3 measured in the upper middle turn of the cochlea after 48 h in culture in controls and after treatment with various concentrations of Mn alone or Mn combined with 20 mM NAD. Downward blue arrows show Mn conditions that were significantly different from control ($p < 0.05$). Horizontal blue arrows show Mn conditions that were significantly different from next higher concentration ($p < 0.05$). Horizon red bars show conditions with Mn + NAD that were significantly ($p < 0.05$) different from Mn of the same concentration. (For interpretation of the references to color in this figure legend, the reader is referred to the web version of the article.)

on SGN and the protection provided by NAD, we counted the number of β-tubulin labeled SGN in a 141.4 μm × 141.4 μm × 5 μm volume (10^5 μm^3) from 8 cochlear cultures (3 locations in each cochlear culture). Fig. 5H shows the mean (SEM, n = 24/group) number of SGN/10^5 μm^3 from the upper middle turn of the cochlea in control cultures and cultures treated for 48 h with various concentrations of Mn alone or Mn plus 20 mM NAD. In control cultures, there were approximately 36 SGNs per 10^5 μm^3. There was a significant treatment effect (One-way ANOVA, F = 12.85, 5 df, $p < 0.0001$) as demonstrated by the fact that SGN densities in the groups treated with the various concentrations of Mn were significantly less than that for the control group (Fig. 5H, Newman–Keuls, $p < 0.05$). There were also significant differences in SGN densities between the 0.5 mM vs. 1 mM groups and the 1 mM vs. 3 mM groups (Fig. 5H, Newman–Keuls, $p < 0.05$). SGN densities in the groups treated with all three concentrations of Mn plus 20 mM NAD were significantly greater than the comparable groups treated with the same dose of Mn alone (Fig. 5H, Newman–Keuls, $p < 0.05$).

3.6. Mn induces TUNEL activation and protection by NAD

Currently, it is not clear which programmed cell death pathway is involved in Mn-induced toxicity in SGN and why NAD can delay this response. To explore these issues, we performed TUNEL staining to determine if the cells within the SGN were dying by apoptosis during the early stages of treatment (9 h duration) with 1.0 mM Mn or Mn plus 20 mM NAD. Illustrated in Fig. 6 are representative confocal images of SGN from the upper middle turn of the cochlea labeled with β-tubulin (red) and TUNEL (green). TUNEL staining (green or yellow) was minimal in control cultures (Fig. 6C) but was frequently observed in SGN cultured for 9 h in 1.0 mM Mn (Fig. 6A). Adding 20 mM NAD to cultures treated with 1 mM Mn reduced the number of TUNEL positive SGN (Fig. 6B). These results suggest that Mn induces apoptosis in SGN and that NAD suppresses the early apoptotic response. To quantify the results, we counted the total number of SGN and the number of TUNEL positive SGN in a 141.4 μm × 141.4 μm rectangular area (optical section thickness 1 μm) in the upper middle turn of the cochlea from control cultures and cultures treated with 1 mM Mn alone or 1 mM Mn plus 20 mM NAD (n = 20 samples/condition); these data were used to determine the mean (±SEM) percentage of TUNEL positive SGN present per 141.4 μM × 141.4 μM area. After 9 h in culture, approximately 4% of SGN were TUNEL positive in controls vs. 38% in cultures treated with 1 mM Mn (Fig. 6D). Adding 20 mM NAD to cultures treated with Mn reduced the percentage of TUNEL positive cells to roughly 16%, more than a 50% reduction in TUNEL positive cells compare to Mn alone. There was a treatment effect for the percentages of TUNEL positive SGN (One-way ANOVA, F = 352. 4, 2 df, $p < 0.0015$) as the percentage of TUNEL positive SGN in the group treated with 1 mM Mn was significantly greater than in controls (Newman–Keuls, $p < 0.05$). The percentage of TUNEL positive SGN in cultures treated with 1 mM Mn plus 20 mM NAD was significantly less than cultures treated with 1 mM alone (Newman–Keuls, $p < 0.05$), but still significantly more than in control cultures (Newman–Keuls, $p < 0.05$).

3.7. NAD suppresses Mn-induce activation of caspase-3, -8, and 9

To investigate the upstream mechanisms underlying Mn-induced apoptosis, we used selective fluorescent probes to detect activated caspase-3, caspase-8 and caspase-9 in control cultures and cultures treated with 1 mM Mn alone or 1 mM Mn plus 20 mM NAD; cultures were evaluated 6 h post-treatment. Representative confocal images of SGN from the upper middle turn of the cochlea are shown in Fig. 7; samples were labeled with β-tubulin and a caspase probe. Caspase-3, caspase-8 and casepase-9 labeling was seldom observed in SGN in control samples. In contrast, caspase-3, caspase-8 and caspase-9 labeling was seen in many SGN in cultures treated with 1 mM Mn for 6 h; caspase labeling occurred

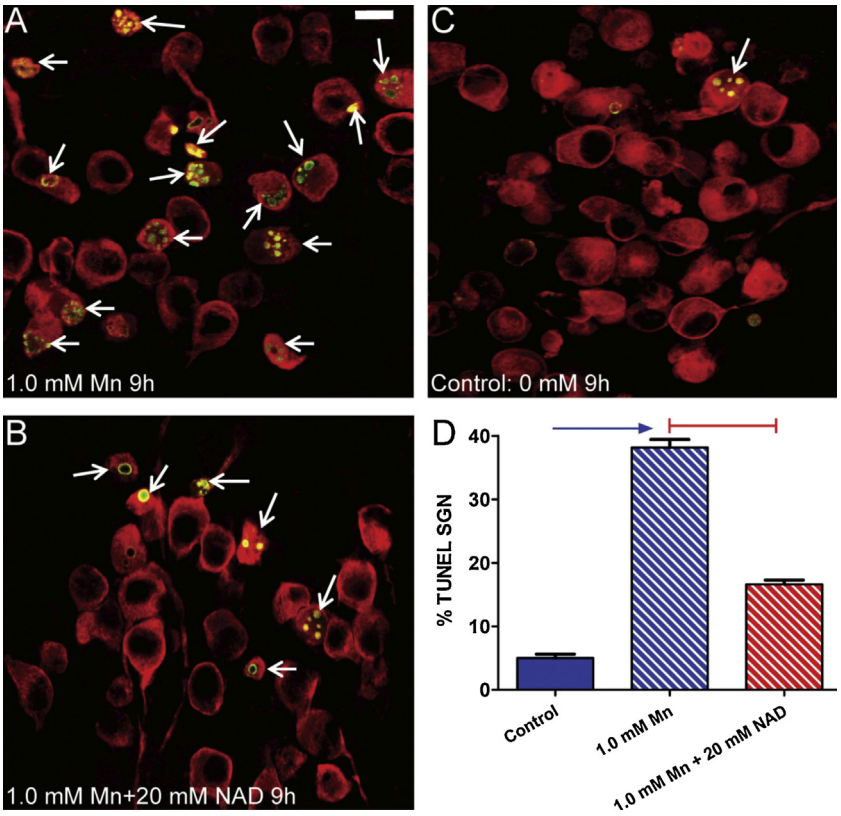

Fig. 6. Representative confocal images showing SGN from upper middle turn of the cochlea labeled for TUNEL (green) and β-tubulin (red) after 9 h in culture; images shown for controls (C) and after treatment with 1 mM Mn alone (A) or Mn combined with 20 mM NAD (B). White arrows point to condensed or fragmented TUNEL stained SGN. Scale bar in (A): 10 μm. (D) Mean ($n = 20$) percentages of TUNEL positive SGN in cochlear organotypic cultures; data shown for controls and samples treated with 1.0 mM Mn alone or Mn combined with 20 mM NAD after 9 h in culture. Double red asterisks show Mn treatment that was significantly different ($p < 0.05$) from control cultures. Single black asterisk shows Mn/NAD treatment that was significantly different ($p < 0.05$) from Mn treatment. (For interpretation of the references to color in this figure legend, the reader is referred to the web version of the article.)

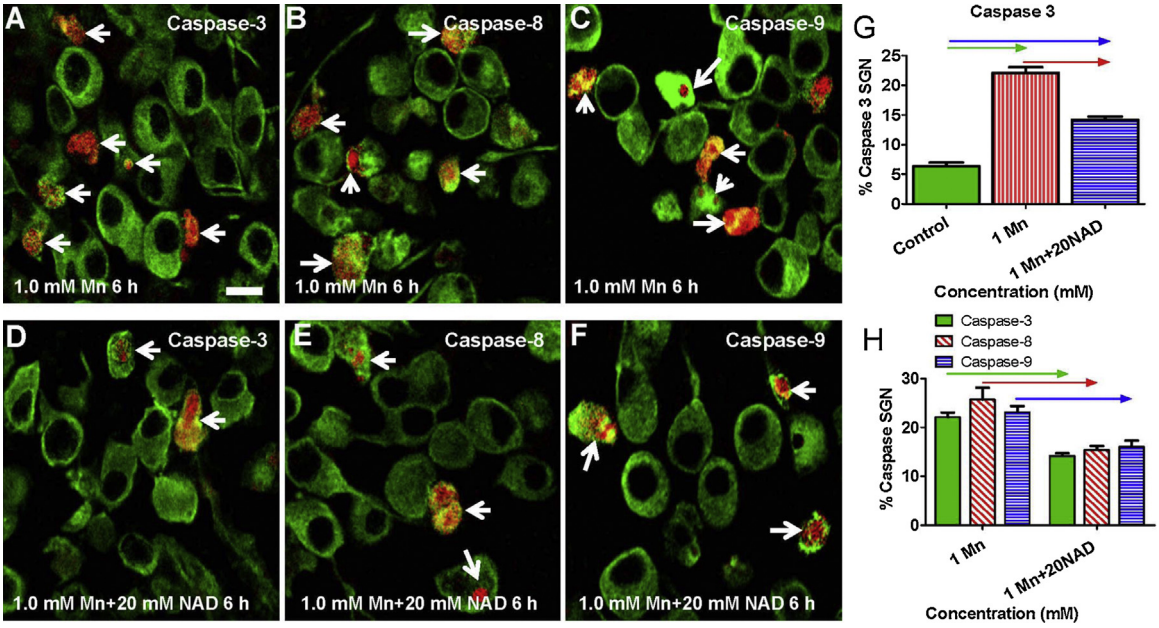

Fig. 7. Representative confocal images showing SGN from upper middle turn of the cochlea. Specimens labeled with red caspase-3 (left column), caspase-8 (middle column) or caspase-9 (right column) and green β-tubulin after 6 h treatment with 1 mM Mn alone (A)–(C) or Mn plus 20 mM NAD (D)–(F). White arrows point to caspase labeled condensed or fragmented SGN. Scale bar in (A): 15 μm. (G) Mean (SEM, $n = 20$) percentages of caspase-3 positive SGN in control cultures and cultures treated with 1 mM Mn or 1 mM Mn plus 20 mM NAD. Arrows shows group differences that were statistically significant from one another (Newman–Keuls, $p < 0.05$). (H) Mean (SEM, $n = 20$) percentages of caspase-3, caspase-8 and caspase-9 positive SGN in cochlear organotypic cultures treated for 6 h with 1.0 mM Mn alone or Mn combined with 20 mM NAD. Arrows show group differences that were significantly different from one another (Newman–Keuls, $p < 0.05$). (For interpretation of the references to color in this figure legend, the reader is referred to the web version of the article.)

predominantly in SGN with shrunken and/or distorted soma (arrows, Fig. 7A–C). With 1 mM Mn plus 20 mM NAD, there was a noticeable reduction in caspase-3, caspase-8 and caspase-9 labeling compared to 1 mM Mn alone (compare Fig. 7D–F with A–C).

We quantified the treatment-dependent changes for caspase-3 by counting the total number of SGN and the number of caspase-3 positive SGNs in 141.4 μm × 141.4 μm rectangular area (optical section thickness 1 μm) from 8 cochlear cultures (2–3 locations in the middle third of each cochlear culture); these data were used to calculate the percentages of caspase-3 positive SGNs in control cultures and cultures treated with 1 mM Mn alone or 1 mM Mn plus 20 mM NAD. As shown in Fig. 7G, the mean (±SEM) percentages of caspase-3 positive SGN were approximately 6, 22 and 14 in control cultures, cultures treated with 1 mM Mn alone and cultures treated with 1 mM Mn plus 20 mM NAD, respectively. There was a main effect of treatment (One-way ANOVA, $F = 116.0$; 2 df, $p < 0.023$). A Newman–Keuls post hoc analysis showed a statistically significant difference between controls and the 1 mM Mn group and between the 1 mM Mn group and group treated with 1 mM Mn plus 20 mM NAD ($p < 0.05$). We also compared the expression of caspase-3, caspase-8 and caspase-9 labeling in cultures treated with Mn alone and those with Mn plus 20 mM NAD by counting the total numbers of SGN and the numbers of caspase positive SGNs in 141.4 μm × 141.4 μm rectangular area (optical section thickness 1 μm) from 8 cochlear cultures (2–3 locations in the middle third of each cochlear culture). In cultures treated with 1 mM Mn alone, approximately 20–27% of SGN were immunopositive for caspase-3, caspase-8 or caspase-9 (Fig. 7H). There was a significant treatment effect (2-way ANOVA, $F = 33.35$, 2 df, $p < 0.0001$) with the percentages of caspase-3, caspase-8 and caspase-9 positive SGN in the groups treated with 1 mM Mn plus 20 mM NAD being significantly less than those in the groups treated with 1 mM Mn alone (Newman–Keuls post hoc analysis, $p < 0.05$). Although there were slightly more caspase-8 positive cells than caspase-9 or caspase-3 positive cells, these differences were not significant.

4. Discussion

Several papers over the past decade have alluded to the correlation between Mn toxicity and Parkinson's disease (Calne et al., 1994; Dobson et al., 2004; Olanow, 2004; Pal et al., 1999). Although Mn toxicity displays similar symptoms as Parkinson's disease, the two disorders differ in several respects including the neurological and cognitive symptoms expressed, the pathophysiology of the disorders and therapeutic management (Roth, 2006). Besides the most prominent neurological concerns, recent studies have also reported that Mn over-exposure can cause ototoxicity (Bouchard et al., 2008; Josephs et al., 2005; Khalkova and Kostadinova, 1986; Korczynski, 2000). The results of the present study using cochlear organotypic cultures confirm our previous finding that Mn exposure can induce significant loss of HC, ANF and SGN within the inner ear (Ding et al., 2011) in a concentration dependent manner. Consistent with these prior studies, the results reported herein demonstrate a selective toxic response to Mn in that lower dose of Mn (0.5–1.0 mM) induced significant degenerative changes to IHC but had little effect on the OHC; however, this difference largely disappeared at the highest concentration (3 mM) consistent with our earlier findings (Ding et al., 2011).

Mn has been reported to accumulate in the inner ear upon acute exposure (Ma et al., 2008). Transport of Mn is normally dependent on divalent metal transporter 1 (DMT1) which is largely responsible for its uptake into neurons and astrocytes. Hair cells share similarities with astrocytes as it has been reported that these cells contain the astrocytic marker, GFAP (Moriya et al., 1993). In addition, gene expression studies indicate that the inner ear contains DMT1 (Ma et al., 2008), consistent with our preliminary immunolabeling studies (in preparation), which may be responsible for differential uptake of Mn into the various cells comprising the inner ear. Differences in the distribution of DMT1 in these cells may be responsible for the selective toxic responses observed upon treatment with Mn.

The data presented in this paper demonstrate for the first time that Mn induces SGN cell death by apoptosis. Mn caused a significant increase in TUNEL staining, which is indicative of DNA fragmentation by labeling the terminal end of nucleic acids, a hallmark feature of cells undergoing apoptosis. During the early stage of treatment (6 h post-treatment), Mn activated the extrinsic, initiator caspase-8 and intrinsic initiator caspase-9, which results from mitochondrial damage and subsequent cytochrome c release and activation of downstream executioner caspase-3 (Deng et al., 2013; Ding et al., 2010; Ryter et al., 2007). While there was slightly more caspase-8 and caspase-9 labeling than caspase-3, these differences were not significant 6 h after Mn treatment. Mn-induced effects on mitochondria and the subsequent generation of oxidative stress signals, which can be prevented by antioxidants, are likely to be responsible for the death of cells within the inner ear.

Several studies have reported that NAD can protect cells against the toxic action of a variety of factors and agents (Belenky et al., 2007; Sauve, 2008). Prior studies from our laboratory demonstrated that 20 mM NAD significantly reduced neuronal degenerations and hair cell loss as well as promoted auditory nerve fiber survival in rat cochlear organotypic cultures incubated with 50 μM oxaliplatin which has been reported to cause hearing loss (Ding et al., 2012). Similarly, NAD was reported to prevent mefloquine-induced neuroaxonal and hair cell degeneration through reduction of caspase-3-mediated apoptosis in cochlear organotypic cultures (Ding et al., 2013). In the present study, NAD was similarly shown to protect against Mn induced toxicity of HC, ANF and SGN within the inner ear thus demonstrating a promising treatment for the mitigation of Mn toxicity. NAD was found to protect both hair and nerve cells at the two lowest concentrations of Mn used and had a greater protective effect on nerve cells at the highest concentration of Mn (Belenky et al., 2007; Sauve, 2008). The mechanism of NAD's neuroprotection in delaying cell toxicity, however, is not fully understood.

Decreased NAD levels are known to activate apoptotic signaling pathways and to stimulate cell death, while an increase can protect against oxidative injury generated by loss of mitochondrial function (Siegel and McCullough, 2011; Zheng et al., 2013). Loss of mitochondrial function is also demonstrated by the observation that treatment with NAD can prevent cell death by inhibiting ATP (Wani et al., 2013). The fact that Mn can also suppress ATP levels (Brouillet et al., 1993; Chen and Liao, 2002; Roth et al., 2000) suggests that NAD protection against Mn-induced cochlear damage may partially be produced by inhibition of ATP loss. NAD protection against Mn-induced cell death may also involve a number of mechanisms besides preserving mitochondrial function and the subsequent generation of apoptotic signals as it also regulates DNA repair via its activation of PARP (poly ADP-ribose polymerase), a protein involved in DNA repair and programmed cell death (Diaz-Hernandez et al., 2007; Oliver et al., 1999; Piskunova et al., 2008; Siegel and McCullough, 2011). Since Mn has previously been reported to stimulate PARP cleavage (Schrantz et al., 1999), it is possible that addition of NAD may also have suppressed this cytotoxic process. These findings are consistent with the results reported in this paper demonstrating that NAD blocked Mn-induced apoptosis as indicated by its effect on DNA fragmentation of SGN as well inhibition of caspase-3, -8 and, -9. These results add further credence to the beneficial effects of NAD in preventing DNA damage and cell apoptosis. As ROS generation and glutamate-mediated excitotoxicity occur with Mn neurotoxicity (Benedetto et al., 2009;

Gavin et al., 1999; Hazell, 2002; Milatovic et al., 2009), the abolishment of cell apoptosis and DNA fragmentation by NAD may be related to its suppression of ROS caused by mitochondrial degeneration. Since niacin provides the most important source of NAD for the human body, there may be possible extra benefits of niacin supplementation in occupations in which exposure to Mn poses a possible threat. In fact, the precursor of NAD, nicotinamide, has previously been shown to protect cells against oxidative stress (Chong and Maiese, 2008; Kang and Hwang, 2009). Consistent with this is the observation that depletion of the coenzyme NAD result in axonal degeneration (Kaneko et al., 2006; Sasaki et al., 2006) whereas supplementation with NAD suppresses axonal degeneration produced by traumatic injury, ischemia damage, autoimmune encephalomyelitis, p53-induced neuron apoptosis and radiation-induced immunosuppression (Klaidman et al., 2003; Luo et al., 2001; Sadanaga-Akiyoshi et al., 2003).

In conclusion, our results reveal that Mn can cause significant toxicity to HC, ANF and SGN. The pathophysiology of Mn toxicity in HC, ANF and SGN is due in part to the upregulation of caspase3-, -8 and -9, DNA fragmentation and induction of apoptosis. At this point it is difficult to directly equate Mn-induced ototoxicity to that which occurs in the basal ganglia, however, based on prior studies in our laboratory (Ding et al., 2011) with organotypic cultures, the sensitivity of the cochlea to Mn is comparable to that of the basal ganglia although the magnitude of the traumatic response is cell specific. Similar to the globus pallidus, GABAminergic neurons are also present in the cochlea further suggesting that Mn may induce a comparable toxic response. In addition, it was shown that NAD suppresses Mn-induced upregulation of caspases, DNA fragmentation and apoptosis thereby enhancing cell survival. These results suggest that precursors of NAD may be effective treatment for Mn intoxication although further studies are warranted to explore the mechanism by which NAD suppresses Mn-induced toxicity to cells within the inner ear.

Conflict of interest

The authors declare that there are no conflicts of interest.

Acknowledgements

Research supported in part by a grant from the National Institute for Occupational Safety and Health, R01 OH010235. The funding sources had no involvement with the experiment or preparation of the manuscript. LW partly supported by China Scholarship Council.

Appendix A. Supplementary data

Supplementary data associated with this article can be found, in the online version, at http://dx.doi.org/10.1016/j.neuro.2013.11.007.

References

Alano CC, Ying W, Swanson RA. Poly(ADP-ribose) polymerase-1-mediated cell death in astrocytes requires NAD^+ depletion and mitochondrial permeability transition. J Biol Chem 2004;279:18895–902.

Belenky P, Bogan KL, Brenner C. NAD^+ metabolism in health and disease. Trends Biochem Sci 2007;32:12–9.

Benedetto A, Au C, Aschner M. Manganese-induced dopaminergic neurodegeneration: insights into mechanisms and genetics shared with Parkinson's disease. Chem Rev 2009;109:4862–84.

Bouchard M, Mergler D, Baldwin M, Panisset M, Bowler R, Roels HA. Neurobehavioral functioning after cessation of manganese exposure: a follow-up after 14 years. Am J Ind Med 2007;50:831–40.

Bouchard M, Mergler D, Baldwin ME, Panisset M. Manganese cumulative exposure and symptoms: a follow-up study of alloy workers. Neurotoxicology 2008;29:577–83.

Bowler RM, Roels HA, Nakagawa S, Drezgic M, Diamond E, Park R, et al. Dose–effect relationships between manganese exposure and neurological, neuropsychological and pulmonary function in confined space bridge welders. Occup Environ Med 2007;64:167–77.

Brouillet EP, Shinobu L, McGarvey U, Hochberg F, Beal MF. Manganese injection into the rat striatum produces excitotoxic lesions by impairing energy metabolism. Exp Neurol 1993;120:89–94.

Calne DB, Chu NS, Huang CC, Lu CS, Olanow W. Manganism and idiopathic parkinsonism: similarities and differences. Neurology 1994;44:1583–6.

Chen CJ, Liao SL. Oxidative stress involves in astrocytic alterations induced by manganese. Exp Neurol 2002;175:216–25.

Chong ZZ, Maiese K. Enhanced tolerance against early and late apoptotic oxidative stress in mammalian neurons through nicotinamidase and sirtuin mediated pathways. Curr Neurovasc Res 2008;5:159–70.

Chun HS, Lee H, Son JH. Manganese induces endoplasmic reticulum (ER) stress and activates multiple caspases in nigral dopaminergic neuronal cells, SN4741. Neurosci Lett 2001;316:5–8.

Deng L, Ding D, Su J, Manohar S, Salvi R. Salicylate selectively kills cochlear spiral ganglion neurons by paradoxically up-regulating superoxide. Neurotox Res 2013;24:307–19.

Desole MS, Sciola L, Delogu MR, Sircana S, Migheli R. Manganese and 1-methyl-4-(2′-ethylpheny1)-1,2,3,6-tetrahydropyridine induce apoptosis in PC12 cells. Neurosci Lett 1996;209:193–6.

Desole MS, Sciola L, Delogu MR, Sircana S, Migheli R, Miele E. Role of oxidative stress in the manganese and 1-methyl-4-(2′-ethylphenyl)-1,2,3,6-tetrahydropyridine-induced apoptosis in PC12 cells. Neurochem Int 1997;31:169–76.

Diaz-Hernandez JI, Moncada S, Bolanos JP, Almeida A. Poly(ADP-ribose) polymerase-1 protects neurons against apoptosis induced by oxidative stress. Cell Death Differ 2007;14:1211–21.

Ding D, Allman BL, Salvi R. Review: ototoxic characteristics of platinum antitumor drugs. Anat Rec (Hoboken) 2012;295:1851–67.

Ding D, Jiang H, Salvi RJ. Mechanisms of rapid sensory hair-cell death following co-administration of gentamicin and ethacrynic acid. Hear Res 2010;259:16–23.

Ding D, Jiang H, Wang P, Salvi R. Cell death after co-administration of cisplatin and ethacrynic acid. Hear Res 2007;226:129–39.

Ding D, Qi W, Yu D, Jiang H, Han C, Kim MJ, et al. Addition of exogenous NAD(+) prevents mefloquine-induced neuroaxonal and hair cell degeneration through reduction of caspase-3-mediated apoptosis in cochlear organotypic cultures. PLoS ONE 2013;8:e79817.

Ding D, Roth J, Salvi R. Manganese is toxic to spiral ganglion neurons and hair cells in vitro. Neurotoxicology 2011;32:233–41.

Ding D, Stracher A, Salvi RJ. Leupeptin protects cochlear and vestibular hair cells from gentamicin ototoxicity. Hear Res 2002;164:115–26.

Dobson AW, Erikson KM, Aschner M. Manganese neurotoxicity. Ann N Y Acad Sci 2004;1012:115–28.

Galvani P, Fumagalli P, Santagostino A. Vulnerability of mitochondrial complex I in PC12 cells exposed to manganese. Eur J Pharmacol 1995;293:377–83.

Gavin CE, Gunter KK, Gunter TE. Mn^{2+} sequestration by mitochondria and inhibition of oxidative phosphorylation. Toxicol Appl Pharmacol 1992;115:1–5.

Gavin CE, Gunter KK, Gunter TE. Manganese and calcium transport in mitochondria: implications for manganese toxicity. Neurotoxicology 1999;20:445–53.

Giordano G, Pizzurro D, VanDeMark K, Guizzetti M, Costa LG. Manganese inhibits the ability of astrocytes to promote neuronal differentiation. Toxicol Appl Pharmacol 2009;240:226–35.

Gunter TE, Gavin CE, Aschner M, Gunter KK. Speciation of manganese in cells and mitochondria: a search for the proximal cause of manganese neurotoxicity. Neurotoxicology 2006;27:765–76.

Hazell AS. Astrocytes and manganese neurotoxicity. Neurochem Int 2002;41:271–7.

Hernandez RB, Farina M, Esposito BP, Souza-Pinto NC, Barbosa F Jr, Sunol C. Mechanisms of manganese-induced neurotoxicity in primary neuronal cultures: the role of manganese speciation and cell type. Toxicol Sci 2011;124:414–23.

Hirata Y, Adachi K, Kiuchi K. Activation of JNK pathway and induction of apoptosis by manganese in PC12 cells. J Neurochem 1998;71:1607–15.

Josephs KA, Ahlskog JE, Klos KJ, Kumar N, Fealey RD, Trenerry MR, et al. Neurologic manifestations in welders with pallidal MRI T1 hyperintensity. Neurology 2005;64:2033–9.

Kaneko S, Wang J, Kaneko M, Yiu G, Hurrell JM, Chitnis T, et al. Protecting axonal degeneration by increasing nicotinamide adenine dinucleotide levels in experimental autoimmune encephalomyelitis models. J Neurosci 2006;26:9794–804.

Kang HT, Hwang ES. Nicotinamide enhances mitochondria quality through autophagy activation in human cells. Aging Cell 2009;8:426–38.

Khalkova Z, Kostadinova G. Auditory-vestibular changes in workers in ferrous metallurgy manufacture. Probl Khig 1986;11:134–8.

Klaidman L, Morales M, Kem S, Yang J, Chang ML, Adams JD Jr. Nicotinamide offers multiple protective mechanisms in stroke as a precursor for NAD^+, as a PARP inhibitor and by partial restoration of mitochondrial function. Pharmacology 2003;69:150–7.

Korczynski RE. Occupational health concerns in the welding industry. Appl Occup Environ Hyg 2000;15:936–45.

Latchoumycandane C, Anantharam V, Kitazawa M, Yang Y, Kanthasamy A, Kanthasamy AG. Protein kinase Cdelta is a key downstream mediator of manganese-induced apoptosis in dopaminergic neuronal cells. J Pharmacol Exp Ther 2005;313:46–55.

Lin WH, Higgins D, Pacheco M, Aletta J, Perini S, Marcucci KA, et al. Manganese induces spreading and process outgrowth in rat pheochromocytoma (PC12) cells. J Neurosci Res 1993;34:546–61.

Lucchini R, Albini E, Placidi D, Gasparotti R, Pigozzi MG, Montani G, et al. Brain magnetic resonance imaging and manganese exposure. Neurotoxicology 2000;21:769–75.
Lucchini RG, Albini E, Benedetti L, Borghesi S, Coccaglio R, Malara EC, et al. High prevalence of Parkinsonian disorders associated to manganese exposure in the vicinities of ferroalloy industries. Am J Ind Med 2007;50:788–800.
Luo J, Nikolaev AY, Imai S, Chen D, Su F, Shiloh A, et al. Negative control of p53 by Sir2alpha promotes cell survival under stress. Cell 2001;107:137–48.
Ma C, Schneider SN, Miller M, Nebert DW, Lind C, Roda SM, et al. Manganese accumulation in the mouse ear following systemic exposure. J Biochem Mol Toxicol 2008;22:305–10.
McFadden SL, Ding D, Salvemini D, Salvi RJ. M40403, a superoxide dismutase mimetic, protects cochlear hair cells from gentamicin, but not cisplatin toxicity. Toxicol Appl Pharmacol 2003;186:46–54.
Migheli R, Godani C, Sciola L, Delogu MR, Serra PA, Zangani D, et al. Enhancing effect of manganese on L-DOPA-induced apoptosis in PC12 cells: role of oxidative stress. J Neurochem 1999;73:1155–63.
Milatovic D, Zaja-Milatovic S, Gupta RC, Yu Y, Aschner M. Oxidative damage and neurodegeneration in manganese-induced neurotoxicity. Toxicol Appl Pharmacol 2009;240:219–25.
Moriya K, Sekitani T, Yamashita H. Glial fibrillary acidic protein (GFAP)-like immunoreactivity in the vestibular endorgan of the rat. Acta Otolaryngol Suppl 1993;503:119–20.
Olanow CW. Manganese-induced parkinsonism and Parkinson's disease. Ann N Y Acad Sci 2004;1012:209–23.
Olanow CW, Good PF, Shinotoh H, Hewitt KA, Vingerhoets F, Snow BJ, et al. Manganese intoxication in the rhesus monkey: a clinical, imaging, pathologic, and biochemical study. Neurology 1996;46:492–8.
Oliver FJ, Menissier-de Murcia J, de Murcia G. Poly(ADP-ribose) polymerase in the cellular response to DNA damage, apoptosis, and disease. Am J Hum Genet 1999;64:1282–8.
Pal PK, Samii A, Calne DB. Manganese neurotoxicity: a review of clinical features, imaging and pathology. Neurotoxicology 1999;20:227–38.
Piskunova TS, Yurova MN, Ovsyannikov AI, Semenchenko AV, Zabezhinski MA, Popovich IG, et al. Deficiency in poly(ADP-ribose) polymerase-1 (PARP-1) accelerates aging and spontaneous carcinogenesis in mice. Curr Gerontol Geriatr Res 2008;2008:754190.
Rivera-Mancia S, Rios C, Montes S. Manganese accumulation in the CNS and associated pathologies. Biometals 2011;24:811–25.
Roth JA. Homeostatic and toxic mechanisms regulating manganese uptake, retention, and elimination. Biol Res 2006;39:45–57.
Roth JA, Feng L, Walowitz J, Browne RW. Manganese-induced rat pheochromocytoma (PC12) cell death is independent of caspase activation. J Neurosci Res 2000;61:162–71.
Rovetta F, Catalani S, Steimberg N, Boniotti J, Gilberti ME, Mariggio MA, et al. Organ-specific manganese toxicity: a comparative in vitro study on five cellular models exposed to MnCl(2). Toxicol In Vitro 2007;21:284–92.
Ryter SW, Kim HP, Hoetzel A, Park JW, Nakahira K, Wang X, et al. Mechanisms of cell death in oxidative stress. Antioxid Redox Signal 2007;9:49–89.
Sadanaga-Akiyoshi F, Yao H, Tanuma S, Nakahara T, Hong JS, Ibayashi S, et al. Nicotinamide attenuates focal ischemic brain injury in rats: with special reference to changes in nicotinamide and NAD^+ levels in ischemic core and penumbra. Neurochem Res 2003;28:1227–34.
Sasaki Y, Araki T, Milbrandt J. Stimulation of nicotinamide adenine dinucleotide biosynthetic pathways delays axonal degeneration after axotomy. J Neurosci 2006;26:8484–91.
Sauve AA. NAD^+ and vitamin B3: from metabolism to therapies. J Pharmacol Exp Ther 2008;324:883–93.
Schrantz N, Blanchard DA, Mitenne F, Auffredou MT, Vazquez A, Leca G. Manganese induces apoptosis of human B cells: caspase-dependent cell death blocked by bcl-2. Cell Death Differ 1999;6:445–53.
Siegel C, McCullough LD. NAD^+ depletion or PAR polymer formation: which plays the role of executioner in ischaemic cell death? Acta Physiol (Oxf) 2011;203:225–34.
Wang J, Zhai Q, Chen Y, Lin E, Gu W, McBurney MW, et al. A local mechanism mediates NAD-dependent protection of axon degeneration. J Cell Biol 2005;170:349–55.
Wani WY, Sunkaria A, Sharma DR, Kandimalla RJ, Kaushal A, Gerace E, et al. Caspase inhibition augments dichlorvos induced dopaminergic neuronal cell death by increasing ROS production and PARP1 activation. Neuroscience 2013 in press.
Wei L, Ding D, Salvi R. Salicylate-induced degeneration of cochlea spiral ganglion neurons-apoptosis signaling. Neuroscience 2010;168:288–99.
Ying W, Garnier P, Swanson RA. NAD^+ repletion prevents PARP-1-induced glycolytic blockade and cell death in cultured mouse astrocytes. Biochem Biophys Res Commun 2003;308:809–13.
Zheng T, Xu SY, Zhou SQ, Lai LY, Li L. Nicotinamide adenine dinucleotide (NAD^+) repletion attenuates bupivacaine-induced neurotoxicity. Neurochem Res 2013;38:1880–94.